Pramāṇa – J. Phys., Vol. 27, Nos 1 & 2, July & August 1986, pp. 47–61.
© Printed in India.

Electron transport in rectangular quantum wells

B R NAG

Institute of Radiophysics and Electronics, Calcutta University, 92 A. P. C. Road, Calcutta 700 009

Abstract. Experimental results on low-field and high-field electron transport in rectangular quantum wells are reviewed. The related theory is presented and the experimental results are examined in the light of the theory. It is concluded that although some experimental results are available and the theory of transport has been developed, numerical agreement between theory and experiments has not yet been reached.

Keywords. Electron transport; rectangular quantum wells; low-field electron mobility; high-field electron mobility; energy relaxation; potential profile; scattering probability.

PACS No. 72·20

1. Introduction

Crystal structures may now be grown with one thin layer of one kind of semiconductor sandwiched between two layers of a different kind of semiconductor. An approximate rectangular quantum well is formed in such structures when the thickness of the sandwiched layer is comparable to electron wavelength and the band gap of the outer layers is larger than that of the sandwiched layer. Such quantum wells have many useful properties which have been exploited for the invention of new devices and realization of more efficient conventional devices. Different properties of these wells are being extensively studied experimentally as well as theoretically.

The nature of electron transport in quantum wells is different from that in bulk homogeneous semiconductors. The electron motion in such structures is confined to two dimensions whereas in bulk, electrons have the freedom of three-dimensional motion. The scattering probabilities are altered and depend on the width of the wells. The importance of the various scattering mechanisms is, as a result, different from that in bulk materials. The electron concentration is often so high that degeneracy affects transport significantly. Electrons may also occupy higher sub-bands, and inter-sub-band scattering, in addition to intra-sub-band scattering, may assume importance. Further, the impurities in such structures may be segregated and large electron concentration may be realized without the concomitant increase in the impurity concentration. Effects of electron screening on electron mobility may hence be clearly demonstrated. In some materials the effects of band nonparabolicity become highly significant as the base energy level may be much higher than the conduction band

The author felicitates Prof. D S Kothari on his eightieth birthday and dedicates this paper to him on this occasion.

minimum. These possibilities, in addition to new device applications, make the study of electron transport in quantum wells interesting as well as rewarding.

The first paper on electron mobility in rectangular quantum wells was published by Dingle *et al* (1978). Since then the subject has been growing rapidly. Experiments have been reported and the theory of transport has also been developed. The purpose of the present paper is to review the published results, examine the status of the theory in relation to experiments and identify areas where further work needs to be done.

2. Quantum well structures

Three kinds of quantum well structures are reported in the literature, as shown in figure 1. In one structure (Stormer *et al* 1979), one kind of semiconductor is grown on another kind and the conduction band edges at the interface between the two semiconductors bend due to electrostatic interaction. A quantum well, often approximated by a triangle, is formed in such structures on one side of the interface. In the second kind of wells, (Dingle *et al* 1978) a layer of semiconductor is sandwiched between two layers of another semiconductor and before the band at one interface can bend significantly, the effect of the other boundary becomes significant. The conduction band edge in the sandwiched layer is then a rectangular well with the bottom line curved

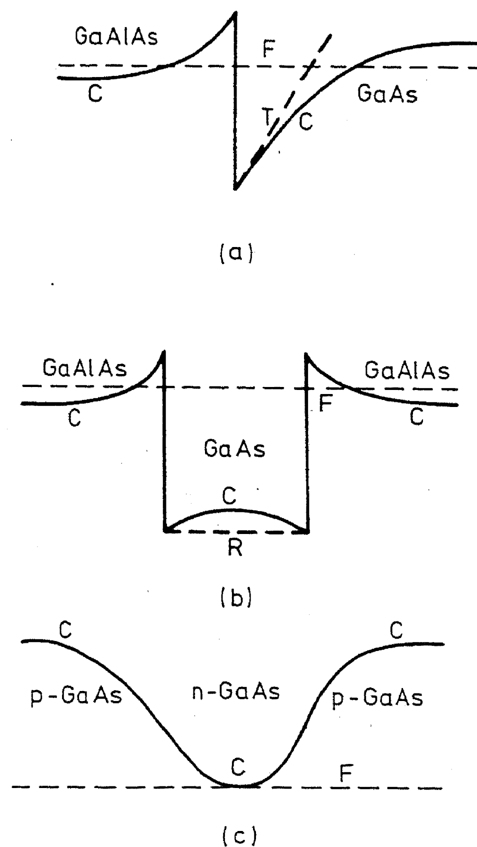

Figure 1. Quantum well systems. **(a)** Heterostructure. **(b)** Rectangular well. **(c)** nipi structure. C, conduction band edge; F, Fermi level; R, rectangular approximation; T, triangular approximation.

upward at the centre. The curving depends on the thickness of the layer and in very thin layers becomes negligible. The third kind (Döhler 1972) of quantum wells is formed by modulating the doping of a semiconductor sample to obtain alternate layers of n and p type. The wells in such structures are approximately rectangular with the bottom curving upward at the edges. In this paper, we shall confine ourselves to the second kind of structure which produces rectangular quantum wells.

The rectangular quantum well structures reported in the literature have been mostly grown by the technique of molecular beam epitaxy by using Ga(x)Al($1-x$)As-GaAs system. The structures are grown on semi-insulating (usually Cr-doped) GaAs substrates. A buffer layer of undoped GaAs (about 1 μm thick) is first grown on the substrate. Layers of GaAlAs and GaAs are then grown alternately with different thicknesses. Some initial studies were made with uniform silicon-doped layers. But, in later studies, the GaAs layer was undoped and the GaAlAs layer was intentionally doped with silicon concentration ranging between 10^{15} cm^{-3} and 10^{18} cm^{-3}. The Fermi level in the GaAs layers in such structures is lower than in the GaAlAs layers and the electrons migrate to the GaAs layers from the GaAlAs layers to align the Fermi levels and produce equilibrium. Under equilibrium, a portion of GaAlAs layer near the interface contain ionized donors, whereas the GaAs layer does not have the impurity atoms but only the electrons. A thin layer of GaAlAs (about 50–150 Å thick) was left undoped in some studies (Störmer *et al* 1981) to act as a buffer between the ionized impurity atoms in the GaAlAs layer and the electrons in the GaAs layer. The structures used in the experiments are of the multiwell type. A number of wells are grown on the same substrate successively, but the thicknesses of the GaAlAs layers are so chosen that there is no interaction between successive wells. The measured conductivity is the resultant of the parallel combination of noninteracting wells.

It should be mentioned that systems using other combinations, e.g., AlInAs-GaInAs and CdTe-InSb have been proposed but detailed experiments on such systems have not yet been carried out. Only a report on the growth of InP-GaInAs structure is available (Razeghi *et al* 1982).

3. Experiments

Experiments have been conducted on electron mobility for low as well as high fields. Experiments have also been conducted to determine energy relaxation time using high fields and optical techniques. We review the results of these experiments in this section.

3.1 *Low-field electron mobility*

In their study on rectangular quantum wells, Dingle *et al* (1978) used Ga(x)Al($1-x$)As with $x = 0{\cdot}7$ and studied mobility in both uniformly-doped and modulation-doped structures at room temperature and also at very low temperatures. The results are illustrated in figure 2. The modulation-doped structures showed a three-fold increase in mobility at liquid helium temperature. The temperature dependence of mobility in uniformly-doped structures is also significantly different from that in bulk material.

A more elaborate experiment on quantum well mobility was performed by Störmer *et al* (1981). They studied the effect of an undoped spacer layer between the doped AlGaAs and undoped GaAs layer. The thickness of the GaAs layer was around 250 Å

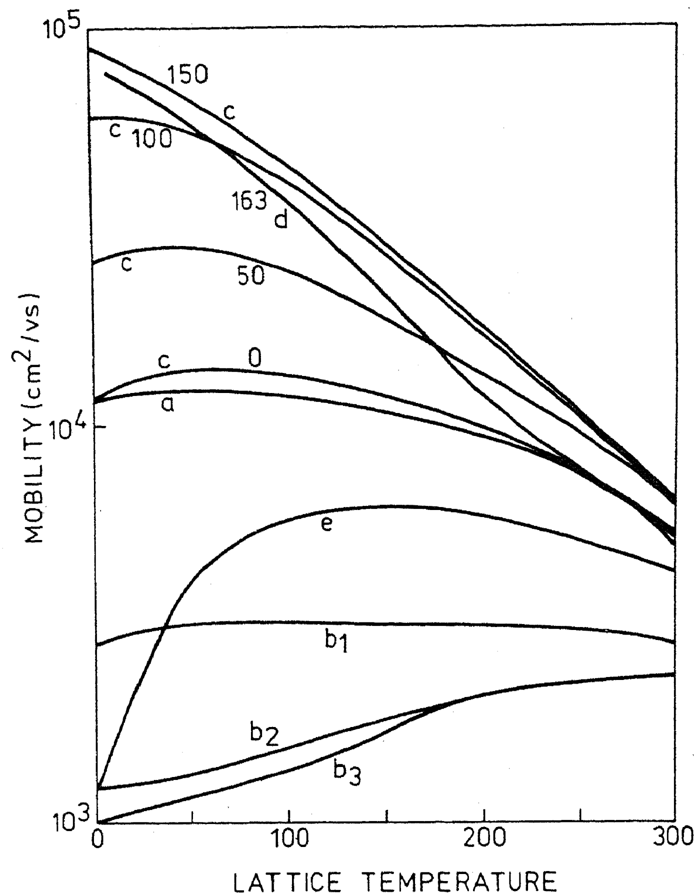

Figure 2. Low-field electron mobility. Curves (a) Modulation-doped (Störmer *et al* 1979). (b) Uniformity doped (Störmer *et al* 1979). ($b_1 - n = 6 \times 10^{17}$ cm^{-3}; $b_2 - n = 1 \times 10^{17}$ cm^3; $b_3 - n = 3 \times 10^{15}$ cm^{-3}). (c) Modulation doped with spacer, numbers indicate spacer thickness in Å (Störmer *et al* 1981). (d) Mobility (Shah *et al* 1984). (e) Bulk.

and the doped GaAlAs layer around 300 Å. Their results are also presented in figure 2. It may be seen that the spacer increases the mobility monotonically at 4·2 K and a value as high as 9·3 m^2/Vs is reached for a spacer thickness of 151 Å. Electron mobility in Al(0·2) Ga(0·8)As (317 Å doped)-Al(0·2)Ga(0·8)As (163 Å-undoped)-GaAs (262 Å-undoped) structures was also studied by Shah *et al* (1983) while studying electric-field-induced heating. The low-temperature low-field mobility was 6·3 m^2/Vs with a carrier density of 7×10^{11} cm^{-2} at 2 K. The mobility remained almost constant upto about 60 K and then monotonically decreased to about 0·63 m^2/V at 300 K. The results are also included in figure 2. The experiment was repeated (Shah *et al* 1984) with Al(0·2)Ga(0·77)As (284 Å doped)-Al(0·23)Ga(0·77)As (118 Å undoped)-GaAs (258 Å undoped) structures. The low-temperature low-field mobility was 9·3 m^2/Vs but the lattice temperature dependence was similar.

No other experiment on electron mobility in rectangular quantum wells is reported in the literature. It would appear that further experiments, using different values of x in Ga(x)Al($1-x$)As, different widths of GaAs layer and other materials, e.g. GaInAs, InSb are needed before definite conclusions may be reached about the limiting values of electron mobility in wells.

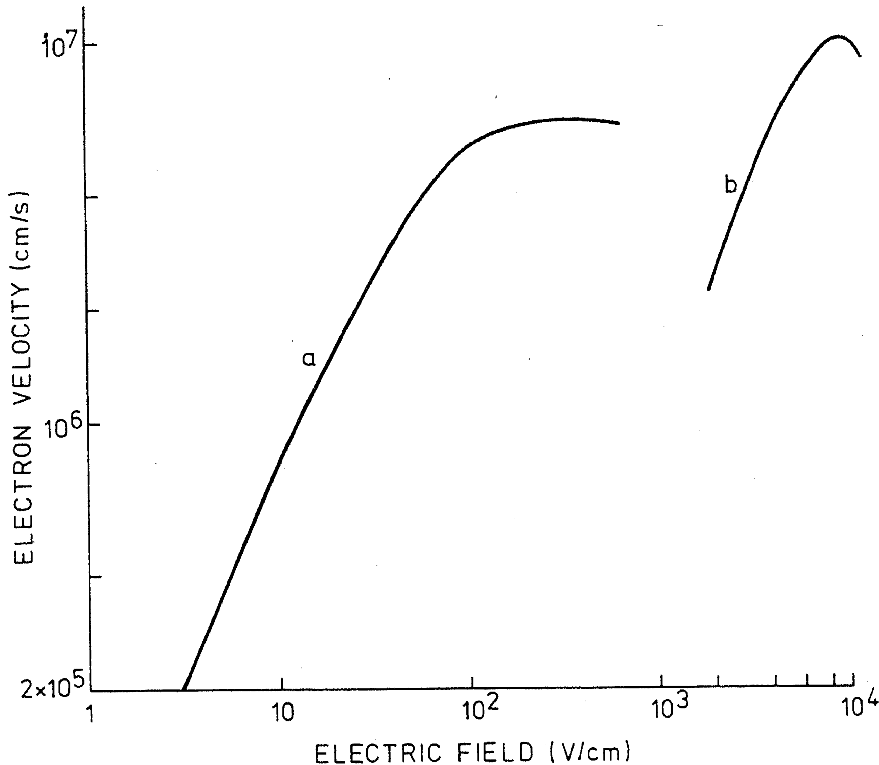

Figure 3. High-field electron velocity. (a) Current density field experiment (Shah *et al* 1984); Lattice temperature: 2 K. Low-field mobility: $7{\cdot}9 \times 10^4\ cm^2/Vs$. (b) Time-of-flight experiment (Höpfel *et al* 1985); Lattice temperature: 300 K.

3.2 *High-field electron mobility*

A number of experiments have been reported on high-field electron mobility in rectangular quantum wells. Wells were realized in one experiment (Höpfel *et al* 1985) by growing 90 Å thick GaAs layers sandwiched between 323 Å unintentionally doped GaAlAs, followed by *p*-doped ($2 \times 10^{18}/cm^3$) 54 Å thick GaAlAs layers. This structure with 20 periods was grown on GaAs substrate. The drift-velocity was obtained by measuring the time-of-flight of photoexcited carriers over distances of 10 μm and 40 μm. The experiment yielded drift velocity of electrons as minority carriers in a *p*-type well with hole concentration of $4{\cdot}2 \times 10^{11}\ cm^{-2}$. The drift velocity increased at low fields linearly with field, reached a maximum value of $1{\cdot}2 \times 10^7$ cm/sec at 8 kV/cm and then decreased with field. The experimental curve is reproduced in figure 3. The drift velocity in the other experiments (Shah *et al* 1983, 1984) was obtained from the current density for different fields using a structure with 258 Å wide wells at a lattice temperature of 2 K. The same experiment was repeated with a different sample. The results of these experiments are also included in figure 3.

3.3 *Energy relaxation of hot electrons*

A number of experiments (Shah *et al* 1983, 1984; Ryan *et al* 1985; Shah *et al* 1985) are reported in which the energy relaxation times of hot electrons in rectangular quantum wells have been measured. The results have a direct bearing on electron transport in quantum wells as insight into electron-phonon interaction may be obtained from these experiments.

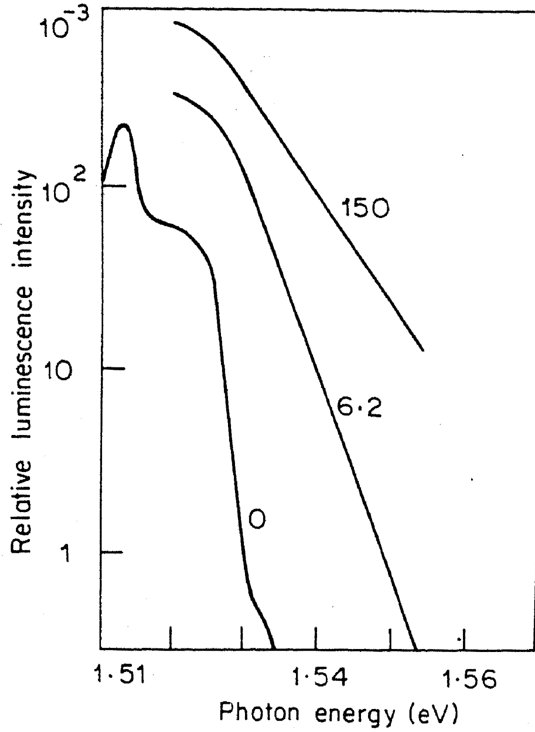

Figure 4. Photoluminescence spectra at 2 K from a doped Al(0·23)Ga(0·77)As-undoped Al(0·23)Ga(0·77)As-GaAs system of 15 periods (Shah *et al* 1983). Thicknesses are respectively 284 Å, 118 Å and 258 Å. Lattice temperature: 2 K. Numbers indicate electric field in V/cm.

Electrons are heated in one set of experiments (Shah *et al* 1983, 1984) by applying an electric field and the photoluminescence spectrum is measured. Such spectra are illustrated in figure 4. It may be seen that the energy tail is Maxwellian and one may deduce the electron temperature from the slope of the luminescence-energy curve. One may obtain the energy relaxation time from the electron temperature and the mobility by using the following relation,

$$|e|\mu\varepsilon^2 = k(T_e - T_L)/\tau_E, \quad (1)$$

where e is the electron charge, μ is the mobility, ε is the electric field, T_e is the electron temperature, T_L is the lattice temperature and τ_E is the energy relaxation time. Two such experiments are reported and the results of one experiment are summarized in table 1. It may be noted that for electron temperatures above about 40 K, the energy loss is mainly through electron-polar-optic-phonon interaction. Under these conditions the energy loss rate may also be expressed as,

$$\frac{\mathrm{d}E}{\mathrm{d}t} = k\frac{\mathrm{d}T_e}{\mathrm{d}t} = \frac{1}{\tau_0}\frac{T_{\mathrm{op}}}{T_e}\exp\left(-\frac{T_{\mathrm{op}}}{T_e}\right), \quad (2)$$

T_{op} being the optic phonon temperature. The constant τ_0 is often taken to be independent of T_e and it may be seen that it is related to τ_E by the relation,

$$\tau_0 = \tau_E(T_{\mathrm{op}}/T_e)\exp(-T_{\mathrm{op}}/T_e). \quad (3)$$

The calculated values of τ_0 are also included in table 1.

Table 1. Energy relaxation time of electrons in a rectangular quantum well (Shah *et al* 1984).

Electric field (V/cm)	Normalized mobility	Electron temperature (K)	τ_E (Picosec)	τ_0 (Picosec)
30	0·87	72	100	1·74
50	0·77	81	45	1·28
100	0·68	100	16	1·01
300	0·37	129	4·2	0·52
500	0·27	139	2·2	0·32
800	0·195	158	1·38	0·25

The carriers are excited by a picosecond light pulse in the second set of experiments (Ryan *et al* 1985; Shah *et al* 1985) and the variation of carrier temperature with time is studied. The time constant τ_0 is determined by fitting the experimental curve to (2). Values of τ_0 are dependent on the energy of exciting phonons. Particularly, when the energy of the photons is such that carriers are excited in both GaAs and GaAlAs layers, τ_0 has a value of 7 psec for 258 Å ($n_{2D} = 5 \times 10^{11}\ \mathrm{cm}^{-2}$) wells. On the other hand, when the energy is such that electrons are excited only in the GaAs layer the value of τ_0 is 1·5 psec, which is of the same order as found in the high-field steady state experiments. The value of τ_0 increases as the well width is reduced to 150 Å ($n_{2D} = 2{\cdot}5 \times 10^{11}\ \mathrm{cm}^{-2}$), although an equation with a single time constant τ_0 does not describe the decay.

4. Theory

4.1 *Potential profile and wave function*

The potential profile in quantum well structures is determined by the discontinuity in the conduction bands and the doping in the constituent layers. As mentioned earlier, the GaAs layer is usually undoped and the GaAlAs layer is doped, both of which are charged due to the movement of the electrons into the GaAs layer from the GaAlAs layer. The exact potential profile can be obtained by solving self-consistently the Poisson equation and the Schrödinger equation for the resulting potentials. However, the charge density in the rectangular quantum well experiments is such that the bending is a small fraction of the potential discontinuity. The theory has therefore been mostly developed by neglecting the bending. Further, even the effect of the finite depth of the potential wells is neglected and the theory so far developed treats the wells to be of infinite height and uses for the solution of the Schrödinger equation the function,

$$\psi = (2/V)^{1/2} \sin(n\pi z/L) \exp(i\mathbf{k}\cdot\rho), \tag{4}$$

where $\mathbf{k}$ is the two-dimensional, (2D) wave vector, ρ is the planar position vector, n is an integer, L is the width of the well in the z-direction, V is the volume of the well.

The energy wave vector dispersion relation is taken as,

$$E = (\hbar^2/2m^*)(k^2 + n^2\pi^2/L^2), \tag{5}$$

where m^* is the effective mass of the electron in GaAs.

4.2 Scattering probability

The theory of electron transport in quantum wells is developed by adapting the theory for transport in bulk materials. The Born approximation and the Boltzmann equation are used. The phonon dispersion relation and the electron-phonon coupling constants are assumed to be identical to those for 3D transport. Only, the integrals are modified by 2D density-of-states. The scattering probabilities for ionized impurity scattering are, however, further modified as the scattering centres outside the well also affect the motion of confined carriers. We quote below the expressions of scattering probabilities for the different kinds of scattering. We note that the general expression for phonon scattering is written as,

$$S(\mathbf{k},\mathbf{k}') = (2\pi/\hbar)|A(q,q_z)|^2|G(q_z)|^2\delta_{\mathbf{k}',\mathbf{k}\pm\mathbf{q}}\delta(E-E'\mp\Delta E) \times (n_{\mathbf{q}}+\tfrac{1}{2}\pm\tfrac{1}{2}), \quad (6)$$

where q is the component of the phonon wave vector in the plane of the well, q_z is the component in the direction of the width of the well, $\mathbf{k}'$, E' and $\mathbf{k}$, E are the values of electron wave vector and energy after and before scattering, $n_{\mathbf{q}}$ is the phonon occupation number, ΔE is the phonon energy, $\mp$ sign corresponds to emission and absorption,

$$G(q_z) = (2/L)\int_0^L \sin(n\pi z/L)\sin(m\pi z/L)\exp(iq_z z)\,\mathrm{d}z, \quad (7)$$

and $A(q,q_z)$ is the part of the matrix-element for electron-phonon scattering containing q and q_z.

It should be noted that the momentum conservation relation is modified to

$$\mathbf{k}' = \mathbf{k} \pm \mathbf{q}, \quad (8)$$

and the q_z component leads to the integral $G(q_z)$, which is often referred to as the overlap integral. The introduction of this term and the difference in the density-of-states term cause the expressions for the scattering probability for 2-D electron gas to be different from that for bulk material.

Electron scattering in rectangular quantum wells by phonons and impurities has been studied by several workers. Deformation potential acoustic phonon scattering was studied by Hess (1979), Price (1981, 1982), Arora and Awad (1981), Ridley (1982) and Kelly (1983). Piezoelectric scattering has been discussed by Price (1981) and Kelly (1983). Polar optic phonon scattering has been evaluated by Hess (1979), Roy *et al* (1981), Price (1981), Ridley (1982), Riddoch and Ridley (1983) and Leburton (1984). Impurity scattering has been analyzed by Hess (1979), Fell *et al* (1978), Lee *et al* (1983) and Mori and Ando (1980). An expression for alloy scattering probability has been derived by Chattopadhyay (1985).

Expressions for the scattering probabilities derived by the various workers are based on the same principles, as outlined earlier. However, the overlap integral $G(q_z)$ has been simplified in different ways and different expressions have been used for the screening constant. In some studies $G(q_z)$ has been taken to be unity (Hess 1979; Roy *et al* 1981). In others, the so-called momentum conservation approximation (MCA) has been used in which $G(q_z)$ is evaluated by assuming that q_z may have the values 0 and $\pm\pi/L$. The

Table 2. Scattering probabilities in a rectangular quantum well.

Kind of scattering	Expression for the scattering probability $S(k)$	Symbols
Acoustic phonon		m^*—Effective mass ratio
(a) Deformation potential	$3m^*E_1^2 kT_L/2\hbar^3\rho_M u^2 L$	E_1—Deformation potential constant
		k—Boltzmann constant
(b) Piezoelectric	$\dfrac{e^2P^2m^*kT_L L}{2\pi\hbar^3\varepsilon_s}\displaystyle\int_0^\pi (x+S)^{-2}F_1(x)\mathrm{d}\theta$	T_L—Lattice temperature
		$\hbar$—Plank's constant/$2r$
		ρ_M—Mass density
Optic phonon:		u—Sound velocity
(a) Non-polar	$3D_0^2m^*(n_0+\frac{1}{2}\pm\frac{1}{2})/4\rho_M\omega_0\hbar^2 L$	P—Piezoelectric constant
		e—Electron charge
(b) Polar	$\dfrac{e^2\omega_0 m^* L}{4\pi\hbar^2\varepsilon_p}\displaystyle\int_0^\pi x^{-2}F_1(x)\mathrm{d}\theta$	ε_s—Static permittivity
Ionized Impurity:		D_0—Optic phonon deformation potential
		ω_0—Optic frequency
(a) Background	$\dfrac{N_I m^*\pi^3L^3e^2}{2\hbar^3\varepsilon_s}\displaystyle\int_0^{\pi/2}\frac{F_2(x_1)\mathrm{d}\theta}{x_1[F_3(x_1)]^2}$	n_0—Optic phonon occupation number
(b) Remote	$\dfrac{N_I m^*\pi^3L^3e^2}{4\hbar^3\varepsilon_s}\displaystyle\int_0^{\pi/2}\frac{(e^{x_1}-1)\exp[-2x_1(L_1/L)]}{[F_3(x_1)]^2}\mathrm{d}\theta$	$\varepsilon_p=\left(\dfrac{1}{\varepsilon_\infty}-\dfrac{1}{\varepsilon_s}\right)^{-1}$
Alloy	$8\pi^2r_0^6E_0^2N_0x(1-x)m^*/3\hbar^3L$	ε_∞—High frequency permittivity
		N_I—Impurity density
	$x=kL\sin\theta,\ x_1=kL\cos\theta,$	r_0—$\sqrt{3/4}\,a_0$
	$F_1(x)=2+\dfrac{x^2}{x^2+4\pi^2}-\dfrac{32\pi^4[1-\exp(-x)]}{x(x^2+4\pi^2)^2}$	E_0—Alloy potential
		a_0—Lattice constant
	$F_2(x_1)=\dfrac{6x_1^5}{\pi^4}+\dfrac{8x_1^3}{\pi^2}+6x_1+\frac{1}{2}[1-\exp(-4x_1)]$	N_0—Number of alloy sites
	$-4[1-\exp(-2x_1)]\left(1+\dfrac{x_1}{2}+\dfrac{x_1^2}{x_1^2+\pi^2}\right)$	L_1—Spacer thickness
	$F_3(x_1)=4x_1^4+x_1^2(4\pi^2+3S)+2\pi^2S$	$S=n_{2D}e^2L/2kT_L\varepsilon_s$

overlap integral has also been evaluated using a delta function to represent the electron (Fell *et al* 1978). The screening constant has been evaluated by using the two-dimensional dielectric function (Mori and Ando 1980, Stern 1967) or by using the function obtained from the Poisson equation according to the Stern-Howard formalism (Hess 1979; Stern and Howard 1967). The impurity potential has been taken to be 2D in some analysis (Fell *et al* 1978), while in others the 3D nature of the potential has been taken into account (Lee *et al* 1983). The matrix elements have been evaluated by using a delta function (Hess 1979; Lee *et al* 1983), a sine function (Lee *et al* 1983) or the wave function for the self-consistent potential distribution (Mori and Ando 1980).

Expressions for the scattering probabilities, obtained by using a sine wave for the electron wave function and a Stern-Howard screening constant are given in table 2. The

different formulae reported in the literature may be obtained by suitably approximating the expressions of table 2.

4.3 *Low-field mobility*

Electron mobility in quantum wells is given by

$$\mu = (|e|/2)\sum_n \int_0^\infty \tau\hbar^{-2}(\partial E/\partial k)^2 (\partial f_{0n}/\partial E)k\, dk[\sum_n f_{0n} k\, dk]^{-1}, \tag{9}$$

where f_{0n} is the distribution function for the electrons in the nth sub-band and τ is the momentum relaxation time. The momentum relaxation time is obtained by using the expressions for the scattering probabilities, noting that for elastic scattering

$$\tau^{-1} = \sum_{\mathbf{k}'} S(\mathbf{k}, \mathbf{k}')(1 - \cos\theta). \tag{10}$$

However, for polar optic phonon scattering, the relaxation time approximation cannot be used and the mobility for predominant polar optic phonon scattering is required to be evaluated by applying the iteration techniques (Nag 1980).

We note that although the formulae for the evaluation of mobility have been discussed in the literature, no detailed numerical results for comparison with experiments are available. However, the temperature dependence and width dependence of impurity-scattering-limited mobility have been studied and some of these results are given in figure 5.

4.4 *High-field transport*

It has been discussed earlier that high-field transport in quantum wells was studied experimentally in connection with energy relaxation. Variation of electron mobility with field at different temperatures has been studied only recently (Höpfel *et al* 1985). However, interest in the theory of high-field transport was initiated by Ridley (1982), who predicted from a study of the scattering probabilities that the conductivity characteristics of quantum wells should exhibit scattering-induced negative differential resistance (NDR). It was argued that, because of the step-like density of states, the scattering probability increases enormously as the electron energy crosses the polar optic phonon emission threshold. Hence, as the average energy of the electrons increases with the field, there would be an onset of large emission scattering and the mobility would drop. This prediction was examined by Chattopadhyay and Ghosal (1983) using the displaced Maxwellian formalism and later by Bose *et al* (1984) by the Monte Carlo method. These results are reproduced in figure 6. It may be seen that no NDR was observed in the calculated curves. However, more recently Al-Mudares and Ridley (1985) reported detailed Monte Carlo calculations including *e-e* scattering. The results indicate that scattering-induced NDR may be obtained for some intermediate values of electron concentration. Some of the results are reproduced in figure 7.

The predictions are yet to be experimentally confirmed. In fact, detailed experiments and related calculations on high-field transport in quantum wells would be of interest as the transport characteristics would be significantly different from the bulk characteristics. The step-like density of states, the presence of multilevels and the variability of width should produce new significant phenomena.

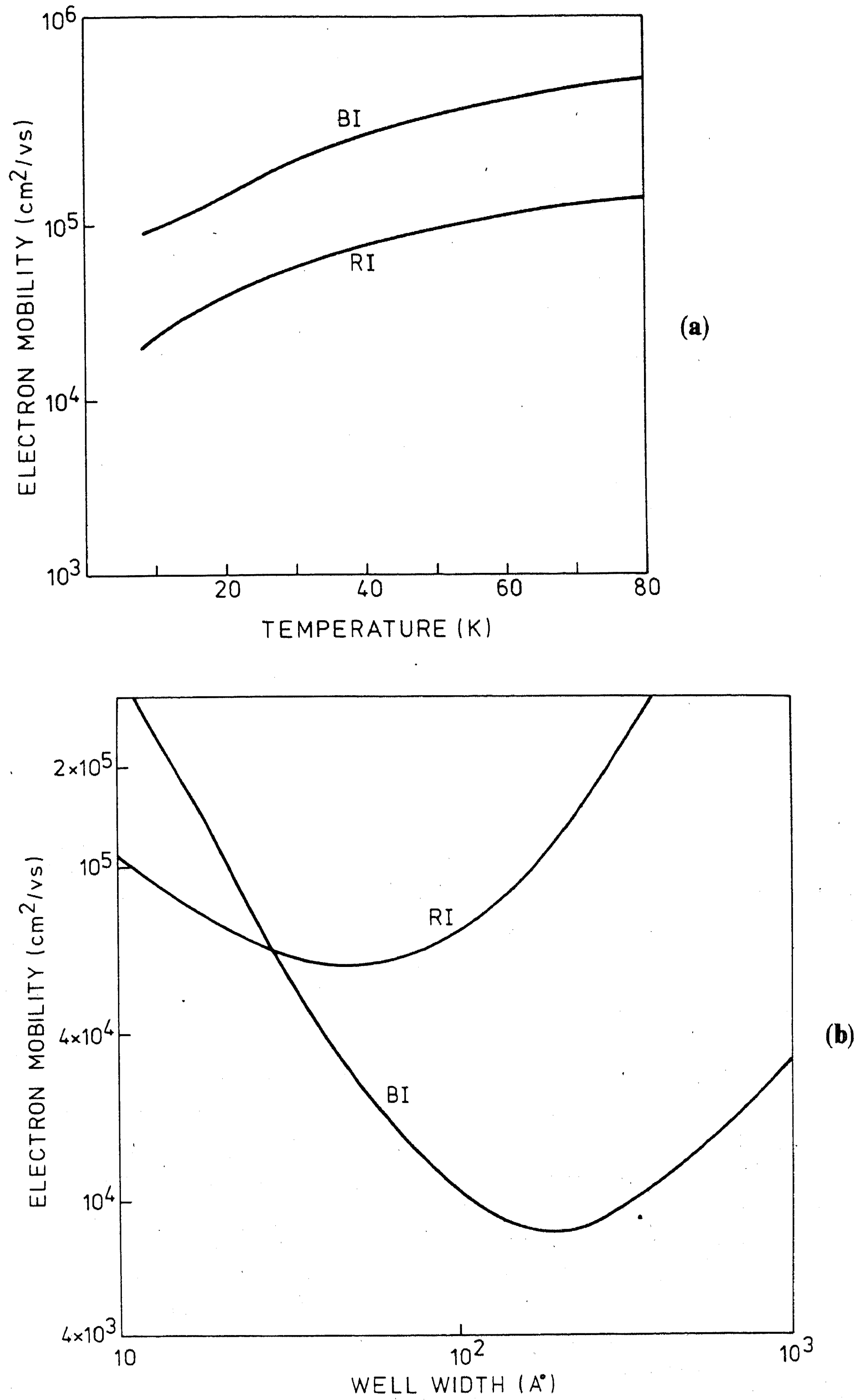

Figure 5. (**a**) Temperature dependence of impurity scattering-limited mobility for a GaAs rectangular well of thickness 100 Å (Lee *et al* 1983); $N_I = 10^{15}\ \mathrm{cm}^{-3}$ and $10^{17}\ \mathrm{cm}^{-3}$ for BI and RI respectively. (**b**) Width dependence of impurity scattering-limited mobility for a GaAs rectangular well with an electron concentration, n_{2d} of $10^{11}\ \mathrm{cm}^{-2}$ (Lee *et al* 1983). BI, background impurities; RI, remote impurities; L: 100 Å.

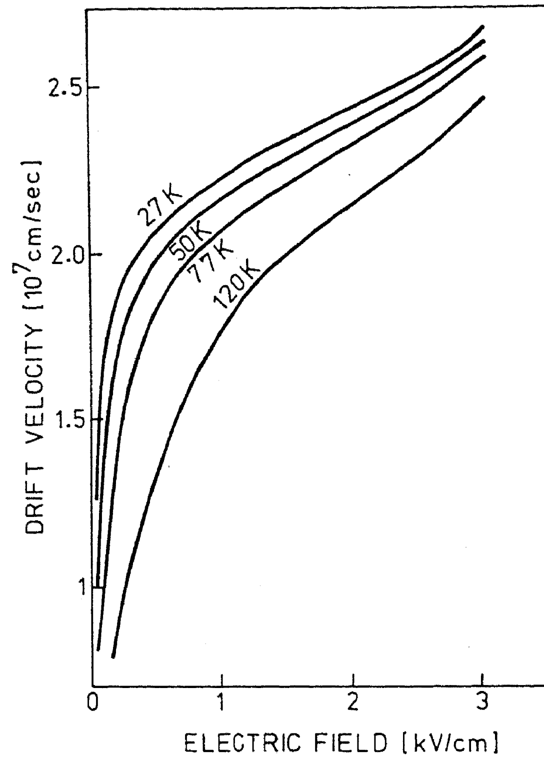

Figure 6. Field dependence of electron velocity in a rectangular GaAs quantum well at different temperatures (Bose *et al* 1983). L: 100 Å.

4.5 *Energy relaxation*

The energy relaxation has been ascribed to be due to polar optic phonon emission for electron temperatures above 40 K. The energy loss rate per electron may then be calculated by using the formula

$$\langle \mathrm{d}E/\mathrm{d}t \rangle = (1/n_{2\mathrm{D}})\hbar\omega_0 \sum_{\mathbf{k},n,\mathbf{k}',m} f_{0n}(\mathbf{k})\,[1-f_{0m}(\mathbf{k}')]\,S(\mathbf{k},\mathbf{k}'). \tag{11}$$

The loss rate calculated for a non-degenerate system by neglecting the screening effects is much larger than the experimental values (Shah *et al* 1983). The values of τ_0 calculated by using the bulk theory are presented in figure 8, along with the values obtained from the experiment. It was suggested that the discrepancy may be due to the effects of degeneracy and screening.

Calculations including the effects of degeneracy and screening have been reported by Basu and Kundu (1985), Das Sharma and Mason (1985), Katayama (1985), and Yang and Lyon (1985). The effects of screening were included by using the dielectric function according to the Lindhard model for 2D electron gas (Ando *et al* 1982). Significant decrease of scattering rate due to screening was found in these calculations and the factor of discrepancy is reduced by about 2 to 3 when screening is included. However, it has been argued by Höpfel *et al* (1985) that the effects of screening cannot be significant as the discrepancy between theory and experiment decreases with increase in temperature and screening is not expected to be sensitive to temperature. The measured values of τ_0 are also not very sensitive to electron or hole concentration. It does appear

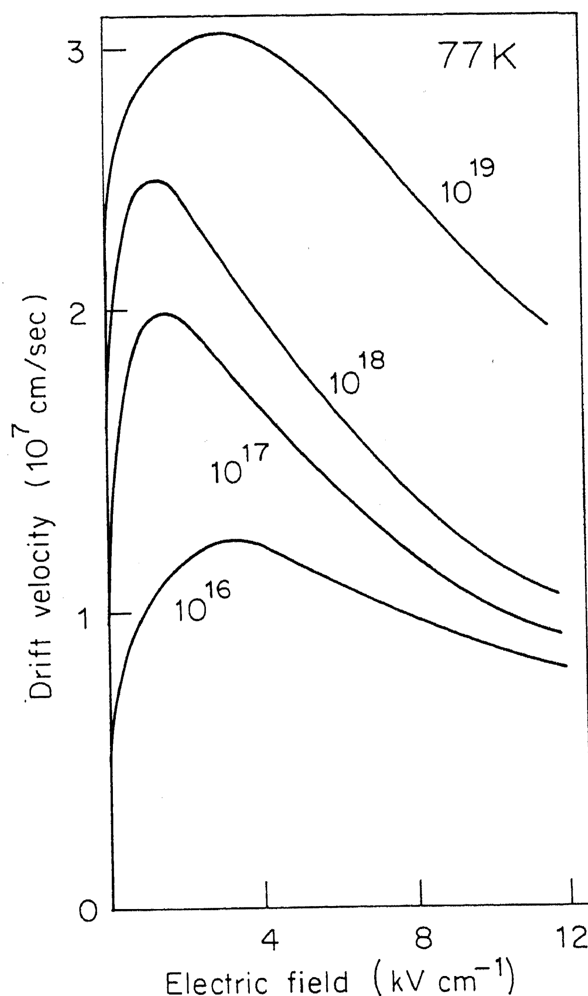

Figure 7. Calculated drift velocity curves for different electron concentration (Al-Mudares and Ridley 1985). *L*: 100 Å.

that a proper evaluation of the screening effect requires a more detailed consideration of the coupled plasmon-phonon modes and associated complexities. On the other hand, the discrepancy may be explained if the hot-phonon effects are included (Price 1985). It is seen that the LO phonons emitted by the electrons are confined within the quantum well as the velocity of such phonons is small. The lifetime of such phonons is about 5–7 psec (Von der Linde *et al* 1980; Kash *et al* 1985) and hence a phonon temperature, much larger than the lattice temperature, may be expected. Calculations including the effects of hot phonons have been reported by Höpfel *et al* (1985). The calculated curve using a value of phonon lifetime of 7 psec is in good agreement with experiments. It should, however, be mentioned that in spite of this agreement, the screening effect will not be negligible and a detailed calculation including degeneracy, screening, hot phonons and non-parabolicity is of importance for explaining the experimental results.

5. Conclusions

The available experimental results on low-field and hot-electron mobility in rectangular quantum wells have been reviewed. The relevant theory has also been presented.

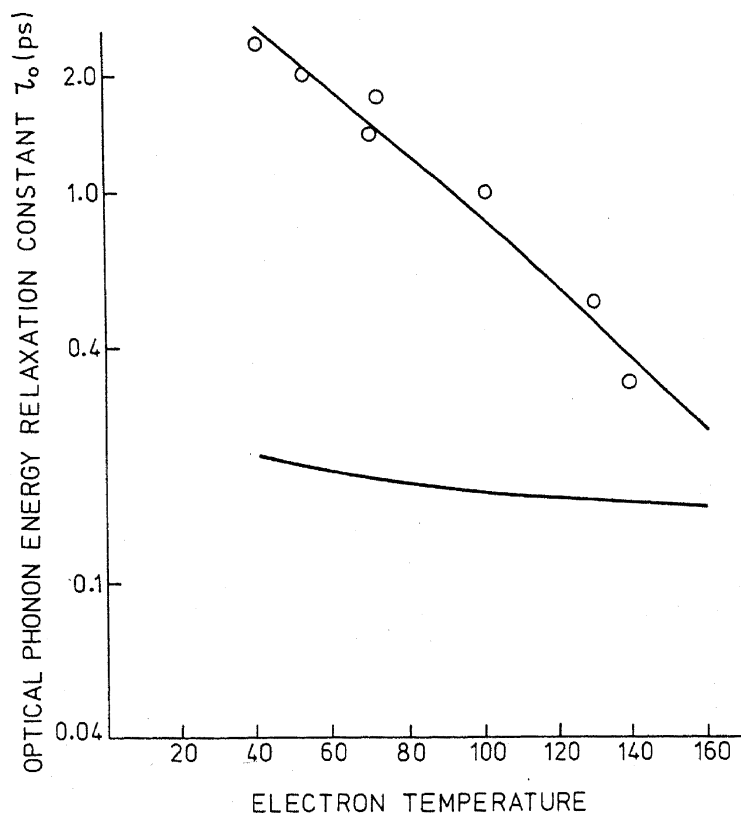

Figure 8. Optical phonon energy relaxation time-constant for different electron temperature (Höpfel *et al* 1985). Upper curve: Experiment. Lower curve: Calculated from 3D theory.

Although the temperature and width dependence of low-field mobility has been studied, a detailed examination of the experimental results in the light of theory is yet lacking. It is also found that detailed experimental as well as theoretical results of hot-electron velocity-field curves are not available.

The studies of hot-electron transport have been aimed at exploring the suggested scattering-induced negative resistance. While conclusions cannot be reached, the possibility of such negative resistance has been indicated. The relevant experiments are also yet to be reported.

Studies have been reported on the energy relaxation rate of hot electrons. The relaxation is mostly due to polar optic phonon scattering above about an electron temperature of 40 K. However, the agreement between theory and experiment is not yet conclusive. Inclusion of hot-phonon effects appears to be necessary for explaining the experimental values of energy relaxation of 2D electrons, which is about 8 times larger than that of 3D electrons.

Acknowledgement

The author is indebted to P K Basu for some helpful discussions.

References

Al-Mudares and Ridley B K 1985 *Physica* **134B** + C 526
Ando T, Fowler A B and Stern F 1982 *Rev. Mod. Phys.* **54** 437
Arora V K and Awad F G 1981 *Phys. Rev.* **B23** 5570
Basu P K and Kundu S 1986 *Surf. Sci.* **170** 526
Bose M, Bose D and Nag B R 1984 *J. Phys.* **C17** 6035
Chattopadhyay D 1985 *Phys. Rev.* **31** 1145
Chattopadhyay D and Ghosal A 1983 *J. Phys.* **C16** 2583
Das Sarma S and Mason B H 1985 *Physica* **134B** + C 301
Dingle R, Störmer H L, Gossard A C and Wiegmann W 1978 *Appl. Phys. Lett.* **33** 665
Döhler G H 1972 *Phys. Status. Solidi.* **B52** 79
Fell B, Chen J T, Hardy J, Prasad M and Fujita S 1978 *J. Phys. Chem. Solids* **34** 221
Hess K 1979 *Appl. Phys. Lett.* **35** 484
Höpfel R A, Shah J, Gossard A C and Wiegmann W 1985 *Physica* **134B** + C 509
Kash J A, Tsang J C and Kvam J M 1985 *Phys. Rev. Lett.* **54** 2151
Katayama S 1986 *Surf. Sci.* **170** 531
Kelly M J 1983 *J. Phys.* **C16** L1165
Leburton J P 1984 *J. Appl. Phys.* **56** 2850
Lee J, Spector H N and Arora V K 1983 *J. Appl. Phys.* **56** 2850
Mori S and Ando T 1980 *J. Phys. Soc. Jpn.* **48** 865
Nag B R 1980 *Electron transport in compound semiconductors* (New York: Springer Verlag) p.153
Price P J 1981 *Ann. Phys.* **133** 217
Price P J 1982 *Surf. Sci.* **113** 199
Price P J 1984 *Phys. Rev.* **B30** 2234
Price P J 1985 *Physica* **134B** + C 164
Razeghi M, Poisson M A, Larivain J P and Duchemin J 1982 *J. Electron. Mater.* **18** 339
Riddoch F A and Ridley B K 1983 *J. Phys.* **C16** 6971
Ridley B K 1982 *J. Phys.* **C15** 5899
Roy J B, Basu P K and Nag B R 1981 *Solid State Commun.* **40** 491
Ryan J F, Taylor R A, Tuberfield A J and Worlock J M 1986 *Surf. Sci.* **170** 511
Shah J, Pinczuk A, Störmer H L, Gossard A C and Wiegmann W 1983 *Appl. Phys. Lett.* **42** 55
Shah J, Pinczuk A, Störmer H L, Gossard A C and Wiegmann W 1984 *Appl. Phys. Lett.* **44** 322
Shah J, Pinczuk A, Gossard A C, Wiegmann W and Kash K 1986 *Surf. Sci.* **170** (to be published)
Stern F 1967 *Phys. Rev. Lett.* **18** 546
Stern F and Howard W E 1967 *Phys. Rev.* **163** 816
Störmer H L, Dingle R, Gossard A C, Wiegmann W and Sturge M 1979 *Solid State Commun.* **29** 705
Störmer H L, Pinczuk A, Gossard A C and Wiegmann W 1981 *Appl. Phys. Lett.* **38** 691
Von der Linde D, Kuhl J and Klingenberg H 1980 *Phys. Rev. Lett.* **44** 1505
Yang C H and Lyon S A 1985 *Physica* **134B** + C 309